



Measurement of anisotropic thermophysical properties of cylindrical Li-ion cells



S.J. Drake ^a, D.A. Wetz ^b, J.K. Ostanek ^c, S.P. Miller ^c, J.M. Heinzel ^c, A. Jain ^{a,*}

^a Mechanical and Aerospace Engineering Department, University of Texas at Arlington, 500 W First St, Rm 211, Arlington, TX 76019, USA

^b Electrical Engineering Department, University of Texas at Arlington, 416 Yates St, Arlington, TX 76019, USA

^c Naval Surface Warfare Center, Carderock Division, U.S. Navy, 1000 Kitty Hawk Ave., Building 77L, Philadelphia, PA 19112, USA

HIGHLIGHTS

- Presents a new method for measuring thermal properties of cylindrical Li-ion cells.
- Results are in excellent agreement with finite-element simulation models.
- Measurements provide cell-level thermal conductivity and heat capacity values.
- Measurements indicate strong anisotropy in thermal conduction.
- Measurements indicate poor radial thermal conductivity.

ARTICLE INFO

Article history:

Received 16 August 2013

Received in revised form

27 November 2013

Accepted 29 November 2013

Available online 11 December 2013

Keywords:

Lithium-ion batteries

Thermal conduction anisotropy

Thermal conductivity

Heat capacity

ABSTRACT

Cylindrical Li-ion cells have demonstrated among the highest power density of all Li-ion cell types and typically employ a spiral electrode assembly. This spiral assembly is expected to cause large anisotropy in thermal conductance between the radial and axial directions due to the large number of interfaces between electrode and electrolyte layers in the radial conduction path, which are absent in the axial direction. This paper describes a novel experimental technique to measure the anisotropic thermal conductivity and heat capacity of Li-ion cells using adiabatic unsteady heating. Analytical modeling of the method is presented and is shown to agree well with finite-element simulation models. Experimental measurements indicate that radial thermal conductivity is two orders of magnitude lower than axial thermal conductivity for cylindrical 26650 and 18650 LiFePO₄ cells. Due to the strong influence of temperature on cell performance and behavior, accounting for this strong anisotropy is critical when modeling battery behavior and designing battery cooling systems. This work improves the understanding of thermal transport in Li-ion cells, and presents a simple method for measuring anisotropic thermal transport properties in cylindrical cells.

© 2013 Elsevier B.V. All rights reserved.

1. Introduction

Several recent incidents, including fire in a Li-ion battery pack aboard an aircraft [1] have highlighted the importance of thermal design of Li-ion batteries. Fundamental studies of thermal phenomena occurring within Li-ion batteries are essential for developing a basic understanding of these technological challenges, and to design cooling systems prevent thermal runaway during high power operation. It is also critical to measure and understand the fundamental thermal transport properties of

a Li-ion cell for accurate system-level modeling and design. Due to the inherently high energy content in Li-ion batteries, thermal phenomena play an important role in performance as well as safe battery operation, and in most cases, contribute to operating limits [2–5]. While electrical and electrochemical phenomena in a Li-ion cell have been widely studied [3,6–10], relatively lesser literature exists on thermal transport in a Li-ion cell. Operation at higher temperatures is known to decompose the electrolyte and thus degrade cell performance and lifetime. If the heat exceeds a critical threshold, which varies upon chemistry type, electrolyte release and fire, and ultimately a cathode thermal runaway situation may arise [11]. Capacity and power reduction has also been found to occur at high operating temperature [12], although lowered impedance and thus increased voltage may offer better output at slightly elevated temperatures.

* Corresponding author. Tel.: +1 817 272 9338; fax: +1 817 272 2952.

E-mail address: jaina@uta.edu (A. Jain).

Fig. 1 shows a top view cutout of a typical Li-ion cylindrical cell. A composite layered material made up of an anode, cathode, separator and current collectors is soaked in electrolyte and rolled in a Swiss roll fashion. Electrode tabs are present at the ends of the cell to collect and conduct electric current to the external cell terminals.

Due to this construction, the nature of radial thermal transport is expected to be significantly different from axial thermal transport. While in the radial direction, heat flow is expected to be impeded by several thermal contact resistances between the thin layers of various, in the axial direction, thermal conduction is expected to occur primarily along the current collector materials, which often run continuously in the axial direction. Thermal contacts between materials in microsystems often present significant thermal resistance, sometimes even greater than the material thermal resistance itself [13]. Due to this expected anisotropy of thermal transport, it is important to experimentally measure the radial and axial thermal conductivities of a cylindrical Li-ion cell, since the assumption of isotropic thermal transport properties in Li-ion cells design will either underpredict or overpredict the temperature field, both of which are undesirable.

Several papers have reported computational and experimental investigation of temperature distribution at the cell-level and at the pack-level [2,3,5,14–17]. Accurate information about underlying thermal properties such as thermal conductivity and heat capacity is critical for the accuracy of such models. However, only a limited set of papers have reported work on thermal property measurement of Li-ion cells. Bandhauer, *et al.* provide a review of thermal phenomena associated with Li-ion cells and also note the lack of thermal property measurement data [18]. Heat capacity measurements of a few batteries using calorimetry have been reported [19]. However, this method does not provide thermal conductivity measurements. A few papers have reported core-to-outside lumped thermal resistance of a cell [14,20], but such a parameter is not particularly useful since not all the heat is generated at the core of a Li-ion cell. Due to the distributed nature of heat generation within a Li-ion cell, it is more appropriate to model the cell using effective thermal conductivity and heat capacity. Maleki, *et al.* have reported measurements of thermal conductivity and heat capacity of Li-ion cells using xenon flash technology (XFT) and steady-state measurements [21]. However, this approach requires two different experiments for measuring thermal conductivity and heat capacity, and more importantly, does not provide thermal conductivity of the cell assembly as a whole. The XFT method is also cumbersome and expensive, and is usually not readily available. Most of the previous

work neglects the anisotropy of thermal conduction within a Li-ion cell. It is desirable to experimentally measure anisotropic components of thermal transport properties in a Li-ion cell. Such work will enhance the accuracy of thermal computation for system-level thermal design, and will also help in developing a fundamental understanding of heat flow within a Li-ion cell.

This paper describes a new method for measurement of effective heat capacity and anisotropic thermal conductivity of cylindrical Li-ion cells. The method described here is relatively simple, and provides rapid measurement of axial and radial thermal conductivity in addition to heat capacity. The method utilizes the thermal response of the cell to axial or radial heating in an adiabatic configuration. An analytical heat transfer model is developed for modeling temperature distribution during such adiabatic heating. It is shown that simultaneous measurement of thermal conductivity and heat capacity can be obtained in a single experiment. Experimental data are in excellent agreement with the analytical model and indicate strong anisotropy in thermal conduction in 26650 and 18650 cells. Results indicate a significant underprediction of peak temperature in using only the axial thermal conductivity compared to a case where the measured anisotropy is accounted for. Results presented in this manuscript will enable more accurate performance models of Li-ion batteries and better designs for battery cooling systems.

2. Experimental method

An experimental technique for determining the heat capacity and anisotropic thermal conductivity of a cell is developed in this work. The technique yields thermal conductivity and heat capacity in a single experiment. In order to do so, the cell is subjected to adiabatic heating in the radial or axial direction, and its temperature rise is measured as a function of time. A flexible Kapton heater is attached to either the curved or top circular surface of the cell, to heat either in the radial or axial direction, respectively. T-type thermocouples are attached at various locations along the cell outer wall to measure temperature. When making radial measurements, thermocouples are attached on the outside surface at mid-cell height. For axial measurements, thermocouples are attached in the center at the two circular ends of the cell. Fiberglass insulation tape is wrapped around the cell to minimize heat loss. All experiments are carried out in a vacuum chamber at -75 kPa (gage) vacuum to further reduce heat loss. The cells are electrically characterized by performing electrochemical impedance spectroscopy (EIS) using a potentiostat, which determines the individual charge and discharge profile of each cell. Using this information, the cells are fully charged prior to testing to avoid variations in lithiation state of the electrode materials and degeneracy in lithium distribution, which might otherwise influence thermal properties. The cell under test is suspended on thin paper arms to minimize thermal conduction loss through surface area contact. To characterize the amount of heat loss through the insulation, one thermocouple is placed outside the insulating tape, and another is suspended in vacuum a small distance from the heater. **Fig. 2(a) and (b)** shows images of the cell with the flexible heater and thermocouples in place inside the vacuum chamber. A Keithley 2612A sourcemeter is used for supplying heating current and measuring voltage. The thermocouple output is sampled at 2 Hz using a National Instruments (NI) 9213 24-bit thermocouple module within an NI cDAQ-9171. Data acquisition is controlled using NI LabVIEW software. Electrical resistance of Kapton heaters used in this work is measured at temperatures between 25 °C and 50 °C. There is less than 0.1% change in resistance, which shows that the temperature coefficient of resistivity is negligible. This ensures constant heat flux into the battery even as the temperature rises. Each



Fig. 1. Top view cutout of a typical Li-ion cylindrical cell.

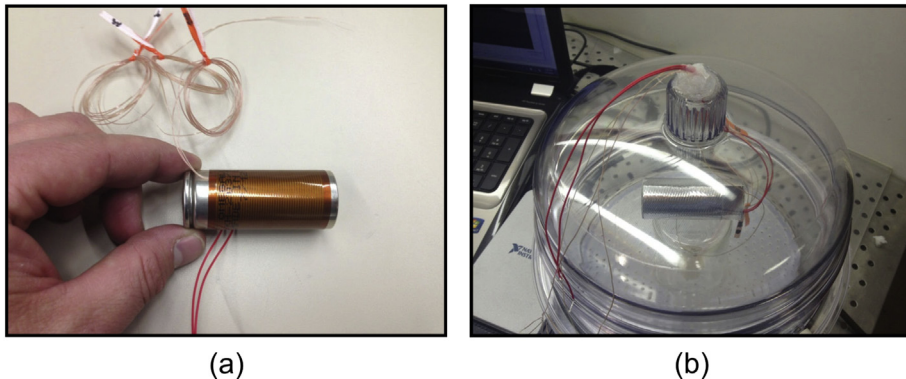


Fig. 2. Images of the experimental setup showing (a) the Li-ion cell with flexible heater and thermocouples, (b) the instrumented Li-ion cell inside a vacuum chamber for thermal measurements.

experiment is stopped once the cell temperature reaches a value that is 10 °C below the manufacturer's rated maximum temperature for the cell. The mass density of each test sample is determined separately by measuring its volume using Vernier calipers and its weight using a scale balance. Mass density of the 26650 and 18650 cells used is measured to be 2285 kg m⁻³ and 2362 kg m⁻³ respectively. Once mass density is known, the experimental setup is used for measuring thermal conductivity and heat capacity of 26650 and 18650 cells. Radial and axial thermal conductivity and heat capacity are determined by comparison with analytical model, which is described next.

3. Analytical model for thermophysical property measurement

This section derives an analytical model for the expected temperature curve as a function of time when a cylindrical Li-ion cell is subjected to radial or axial heating on one of its outer surfaces, while all other surfaces are kept adiabatic. **Fig. 3(a) and (b)** shows a schematic of the geometry for a cylindrical Li-ion cell of radius R and height H being subjected to uniform and steady heat flux Q'' starting at $t = 0$ either in the radial direction at $r = R$, or in the axial direction at $z = H$. In each case, all other boundaries are adiabatic. In order to derive an expression for the temperature of the cell as a function of space and time, governing energy conservation equations along with boundary and initial conditions are written and

solved. For the radial heating case shown in **Fig. 3(a)**, heat flows only in the radial direction. As a result, the temperature distribution is one-dimensional in space. Assuming that the radial thermal conductivity is uniform and independent of temperature, the governing energy equation is

$$\frac{1}{r} \frac{\partial}{\partial r} \left(r \frac{\partial \theta}{\partial r} \right) = \frac{\rho C_p}{k_r} \frac{\partial \theta}{\partial t} \quad (1)$$

where $\theta(r,t)$ is the temperature rise above ambient, and ρ , k_r and C_p are the mass density, radial thermal conductivity, and heat capacity of the cell respectively. Boundary conditions for the temperature distribution are

$$\frac{\partial \theta}{\partial r} = \frac{1}{k_r} Q'' \quad \text{at } r = R \quad (2)$$

$$\frac{\partial \theta}{\partial r} = 0 \quad \text{at } r = 0 \quad (3)$$

It is assumed that the cell is initially at ambient temperature, i.e. $\theta(r,0) = 0$.

Since there is only heat flux into the system, without any mechanism for heat loss, this problem does not have a steady-state solution and theoretically speaking, the temperature of the battery keeps rising as a function of time. In reality, second-order effects such as radiation will limit the temperature rise at very high temperatures. Within the relatively low temperature range in this work, radiation has been shown to be negligible [22]. An expression for $\theta(r,t)$ can be derived by recognizing that the average temperature of the battery, denoted by $\theta_m(t)$ must rise linearly with time. It can be shown that for such problems without a steady-state, the sub-problem resulting from the subtraction of $\theta_m(t)$ from $\theta(r,t)$ has a solution comprising $s(r)$, a steady-state component, and $w(r,t)$, an exponentially decaying transient component.

The average temperature rise $\theta_m(t)$ can be determined by considering the total thermal capacity of the cell mass. By solving the remaining sub-problem using linear superposition and eigenfunctions expansion, the final solution is derived to be

$$\theta(r,t) = \theta_m(t) + s(r) + w(r,t) = \frac{2Q''}{\rho C_p R} t + \frac{Q''}{k_r R} \left(\frac{r^2}{2} - \frac{R^2}{4} \right) - \frac{2Q'' R}{k_r} \sum_{n=1}^{\infty} \frac{J_0(\lambda_n r)}{(\lambda_n R)^2 J_0(\lambda_n R)} \exp \left(-\frac{k_r \lambda_n^2}{\rho C_p} t \right) \quad (4)$$

The eigenvalues λ_n are obtained from roots of the equation $J'_0(\lambda_n R) = 0$. J_0 denotes Bessel function of the first kind of order 0.

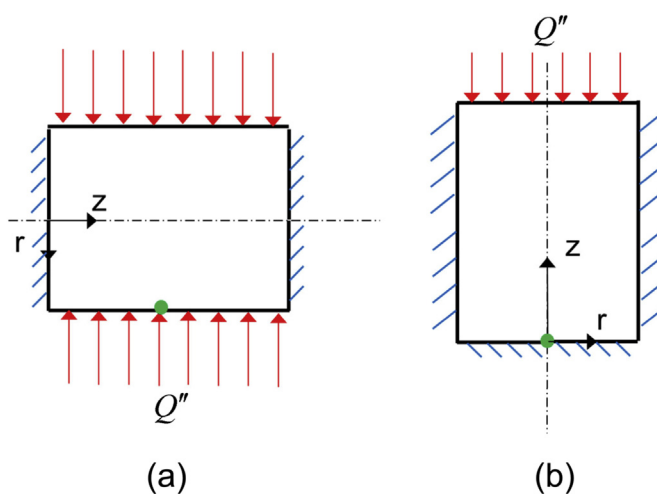


Fig. 3. Schematic of the geometry for the (a) radial heating, and (b) axial heating cases.

Equation (4) shows that the temperature measured at each location has three components – a component that linearly increases with time, for which the slope is inversely proportional to the product ρC_p , a time-invariant, spatially varying term which is inversely proportional to the radial thermal conductivity, and an exponentially decaying term for which the time constant is inversely proportional to the radial thermal diffusivity. Provided the density can be measured separately, this shows that the measurement of the slope and intercept of the temperature curve after transients have died out can be used to simultaneously determine the heat capacity and radial thermal conductivity of the cell under test.

For the axial heating case, temperature profile is expected to be one-dimensional in space due to radial symmetry. Assuming that the axial thermal conductivity is uniform and independent of temperature, the governing energy equation is given by

$$\frac{\partial^2 \theta}{\partial z^2} = \frac{\rho C_p}{k_z} \frac{\partial \theta}{\partial t} \quad (5)$$

where $\theta(z,t)$ is the temperature rise, and k_z is the axial thermal conductivity. Boundary conditions for the temperature distribution are

$$\frac{\partial \theta}{\partial z} = \frac{1}{k_z} Q'' \quad \text{at } z = H \quad (6)$$

$$\frac{\partial \theta}{\partial z} = 0 \quad \text{at } z = 0 \quad (7)$$

It is assumed that the cell is initially at ambient temperature, i.e. $\theta(r,0) = 0$.

This problem is solved in a similar manner as the radial problem. In this case, the solution is found to comprise three components given by

$$\begin{aligned} \theta(z,t) = \theta_m(t) + s(z) + w(z,t) &= \frac{Q''}{\rho C_p H} t + \frac{Q''}{2k_z H} \left(z^2 - \frac{H^2}{3} \right) \\ &+ \sum_{n=1}^{\infty} \frac{(-1)^{n+1} 2Q'' H}{k_z (n\pi)^2} \cos\left(\frac{n\pi z}{H}\right) \exp\left(-\frac{k_z (n\pi)^2}{\rho C_p H^2} t\right) \end{aligned} \quad (8)$$

Measurement of the slope and intercept of the temperature curve at large time results in determination of the heat capacity and axial thermal conductivity respectively.

When designing an experimental setup such as this, it is important to select the sample height, H such that it provides

measurable values of the slope and intercept. If H is too small, the slope is too large, and the temperature rises very rapidly, leading to large experimental uncertainty. This also results in approaching the maximum temperature limit of the cell too soon. On the other hand, if H is too large, both the slope and intercept are small and the time constant of the transient decay is too large, resulting in very sluggish temperature rise as a function of time. If the sample size is fixed, as is the case for a standard Li-ion cell, the heat flux Q'' may be adjusted to result in increased sensitivity of experimental data.

4. Results and discussion

4.1. Analytical model validation

Fig. 4 presents the temperature predicted by the radial model (equation (4)) as (a) a function of time for $r = R$, and (b) as a function of r for $t = 1000$ s. Results from a transient finite-element simulation carried out in ANSYS™ are also shown for comparison. There is excellent agreement between the two. Similar agreement is observed between the axial model (equation (8)) and a finite-element simulation, both as function of time and z , as shown in Fig. 5. The computation time of the analytical model, roughly a few seconds, is much less than the finite-element simulation, roughly several minutes, particularly since there is no set up time needed for modeling and meshing the geometry. Moreover, the analytical model provides a fundamental understanding of the thermal physics that is not apparent from the finite-element simulations. Fig. 4(b) shows a significant temperature gradient within the cell between $r = 0$ and $r = R$ for thermal properties representative of Li-ion cells, as described in the next section. The presence of a temperature gradient within the cell is important to consider when evaluating the electrochemical design and operation of the cell, as well as for modeling of thermomechanical stress generation. Figs. 4 and 5 assume representative values for the thermal properties of the geometry under consideration. Excellent agreement between analytical model and finite-element simulations shown in Figs. 4 and 5 is verified for a typical range of expected values.

4.2. Measured thermophysical properties for 26650 and 18650 cells

Experimentally measured temperature curves for 26650 cell are shown in Fig. 6 for the radial and axial heating tests, measured at mid-height on the outside surface of the cell, $r = R$, and at the end of the cell opposite to the heater, $z = 0$, respectively. Fig. 7 shows similar curves for an 18650 cell. Radial and axial measurements for 26650 as well as 18650 cells are in excellent agreement with the analytical model presented in Section 3, including in the transient

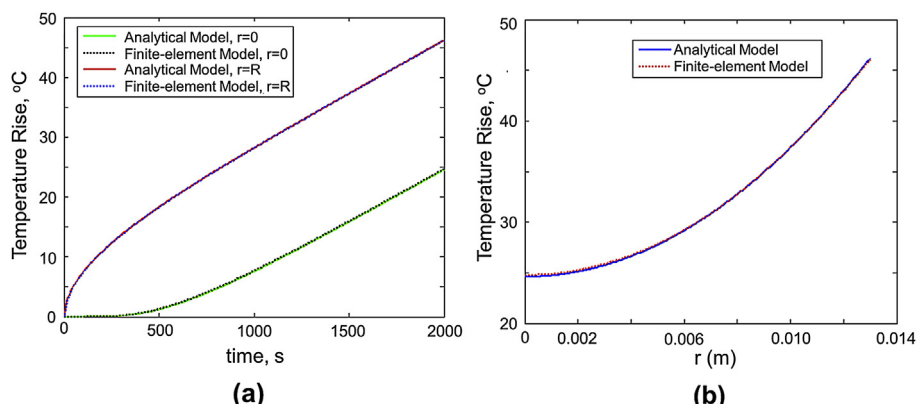


Fig. 4. Comparison of radial model with finite-element thermal simulation.

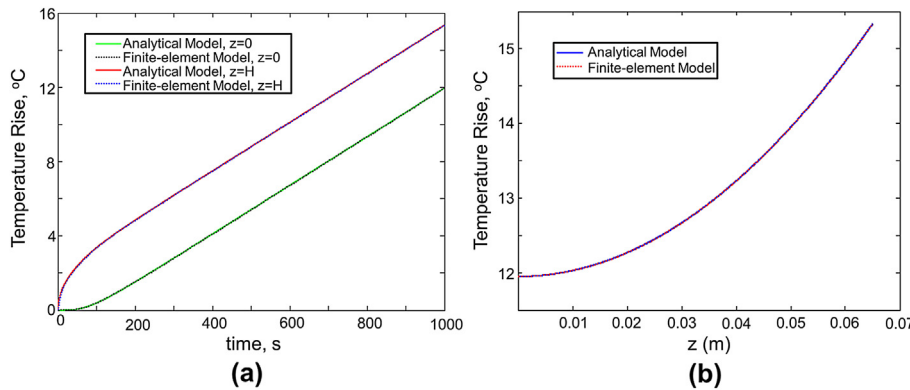


Fig. 5. Comparison of axial model with finite-element thermal simulation.

portion of the temperature curves. As expected from the model, the axial data is concave whereas the radial data is convex. The measured temperature curves comprise a linear term, a constant shift, and an exponentially decaying component. The slope is always positive, whereas the intercept is positive for the radial case, and negative for the axial case. This corresponds to positive and negative values of the second term in equations (4) and (8) respectively. Through comparison of the slopes and intercepts of the temperature curves with analytical model, the radial and axial thermal conductivities of the 26650 and 18650 cells are determined, and are summarized in Table 1. These values are determined such that the mean square error between experimental data and the analytical model is minimized. There is a two orders-of-magnitude difference between the radial and axial thermal conductivities for both 26650 and 18650 cells, indicating strong anisotropy in thermal conduction within the cells. Measured heat capacity for the axial test is somewhat lower than the radial test (e.g., $1605 \text{ J kg}^{-1} \text{ K}^{-1}$ vs. $1895 \text{ J kg}^{-1} \text{ K}^{-1}$ respectively for 26650 cell). The small difference is attributed to the fact that since temperature measurement in the radial experiment is made at the center plane of the cell, $z = 0.5H$, it does not account for the presence of metal tabs at the battery ends. When the metal tabs are taken into account in the axial experiment, the measured heat capacity is somewhat lower due to the lower heat capacity of metals compared

to the organic solvents that constitute the battery electrolyte [23,24]. The axially measured heat capacity is believed to be more accurate due to the tabs being taken into account.

Thermal conductivity values measured in this work are somewhat lower than previous measurements on individual cell constituents such as the electrode-separator assembly that report out-of-plane thermal conductivity of around $1\text{--}3 \text{ W m}^{-1} \text{ K}^{-1}$ [21] and $0.3\text{--}1.6 \text{ W m}^{-1} \text{ K}^{-1}$ [17]. This is possibly because the present experiments take into account multiple thermal contact resistances that exist in an actual cell but not in an isolated sample. By accounting for such thermal contact resistances, measurements reported in this work are expected to be more accurate than previous work. Even though both 26650 and 18650 cells used in this work employ the LiFePO₄ chemistry, there is a small variation in the measured property values. This is possibly because the number of interfacial thermal resistances in the two cells may be slightly different due to the different aspect ratios. Moreover, small variations in the materials and thicknesses for various other components such as metal tabs, container, etc. may also contribute to the small difference between the two.

The measured anisotropy in thermal conductivity originates from the Swiss roll-like arrangement of the anode-separator-cathode inside the cell. Heat flow in the radial direction encounters several material interfaces, whereas in the axial direction, heat

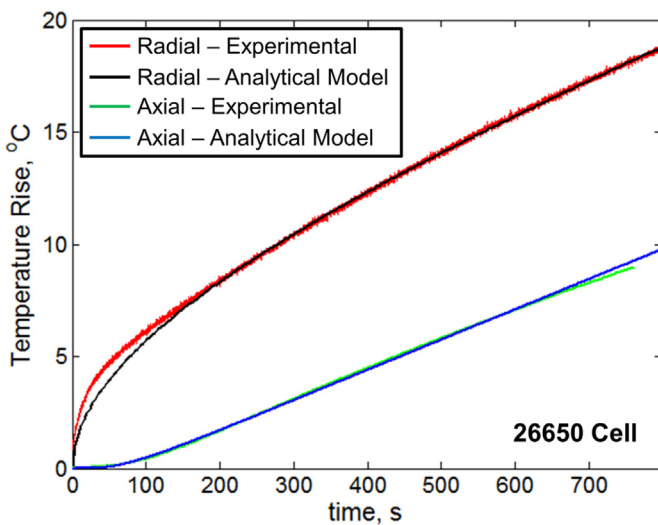


Fig. 6. Comparison of experimental data and analytical model for radial and axial thermophysical property measurements for 26650 cell.

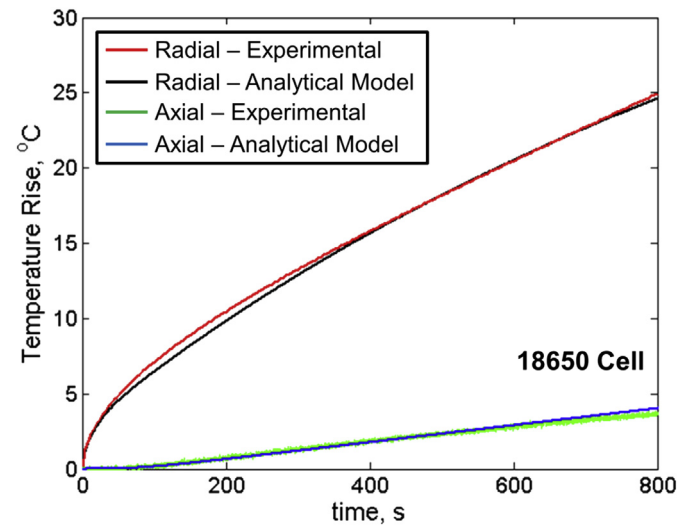


Fig. 7. Comparison of experimental data and analytical model for radial and axial thermophysical property measurements for 18650 cell.

Table 1

Measured thermophysical properties of 26650 and 18650 cells.

	k_r (W m ⁻¹ K ⁻¹)	k_z (W m ⁻¹ K ⁻¹)	C_p (J kg ⁻¹ K ⁻¹)
26650	0.15 ± 0.01	32 ± 1.6	1605 ± 80
18650	0.20 ± 0.01	30.4 ± 1.5	1720 ± 86

flows in mostly a single material without encountering many material interfaces. It is also possible that the thermal conductivities of the anode, separator, and cathode materials might themselves be anisotropic with an out-of-plane thermal conductivity value that is much smaller than the in-plane component. It is well-known that the in-plane thermal conductivity of thin film materials is much higher than the out-of-plane component [13].

The strong anisotropy of thermal conductivity has important implications in thermal design of the cell. Assumption of a single-valued thermal conductivity will result in either severe under-prediction or overprediction of cell temperature depending on whether the axial or the radial thermal conductivity value is used. This is shown in Fig. 8, which compares the temperature contour inside a 26650 cell for the anisotropic case to isotropic cases assuming either the axial or the radial thermal conductivity value. In each case, a constant volumetric heat generation rate within the cell body and a constant convective heat transfer coefficient on the cell surfaces are assumed. The temperature field is determined using a finite-element simulation. Fig. 8 shows that the anisotropic assumption results in a peak temperature rise of 24 K, whereas the isotropic assumption, using the radial and axial thermal conductivity values result in peak temperature rise of 33 and 11 K respectively. Moreover, the isotropic case using the axial thermal conductivity value incorrectly predicts a very uniform temperature distribution within the cell. As a further illustration, simulations are carried out to predict the maximum cell temperature by measuring the outside temperature of the cell. Simulations indicate that if the measured temperature at the cell's outside body is 45 °C at a 25 °C ambient, then an isotropic thermal conductivity

model assuming a value equal to the radial or axial thermal conductivity will predict a core temperature of 78 °C or 46 °C, whereas the correct core temperature, determined using an anisotropic thermal conductivity model will be 74 °C. The temperature contours predicted by the isotropic models will also be incorrect.

While the first isotropic case described above will lead to unnecessary overdesign of the thermal solution, the other case might lead to safety problems due to under-prediction of peak temperature. The use of anisotropic thermal conductivity with accurately measured values is most appropriate for thermal design of the cell. It is also important to consider thermal conduction anisotropy in multi-physics cell design where other physical phenomena such as electrochemical reaction kinetics, charge/discharge rates, mechanical stresses, etc. depend on the temperature distribution. When such phenomena are themselves space-dependent within the cell, it is important to accurately predict the spatial temperature distribution by recognizing the anisotropy in the thermal conductivity.

4.3. Experimental uncertainty analysis

T-type thermocouples used in the current work are accurate to 0.25 °C, which contributes approximately 2% uncertainty in thermophysical property measurements. Other measurements such as geometry, electric current, voltage, etc. have much lower relative uncertainty. Uncertainty in thermophysical property measurements may arise from heat loss into the insulating layer surrounding the test cell. Since all tests described in this paper are transient in nature, heat generated in the heater, whether axial or radial, flows either into the cell, or into the surrounding insulation layer. The ratio of heat flows to the two thermal capacitors is given by the ratio of their thermal masses. Thus

$$\frac{Q_{\text{insulation}}}{Q_{\text{cell}}} = \frac{(m \cdot C_p \cdot \frac{d\theta}{dt})_{\text{insulation}}}{(m \cdot C_p \cdot \frac{d\theta}{dt})_{\text{cell}}} \quad (9)$$

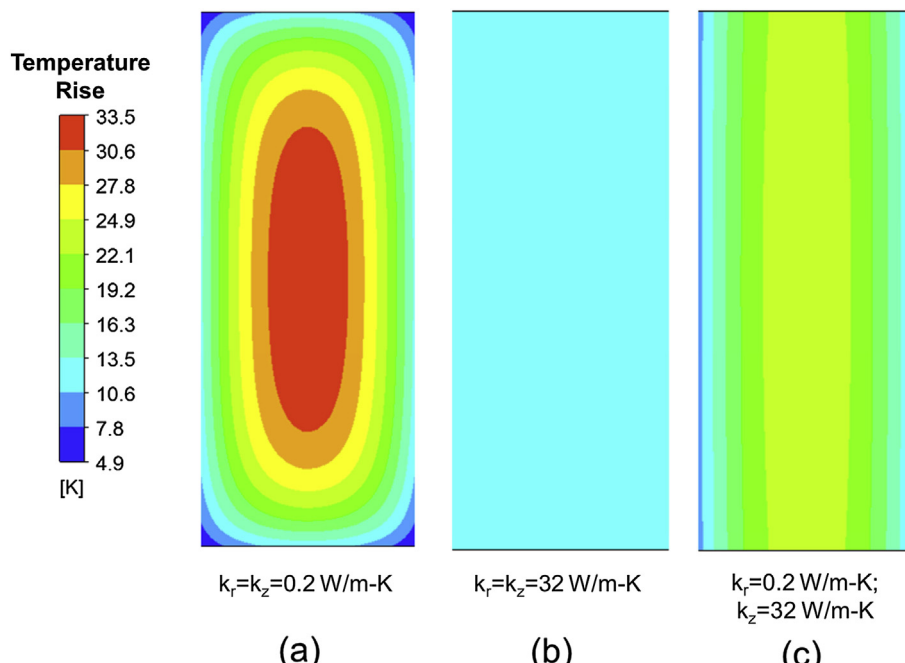


Fig. 8. Simulations results showing the effect of the nature of thermal conductivity on expected temperature profile within a 26650 cell. Panels (a) and (b) are with isotropic thermal conductivity, assuming either the measured (a) radial or (b) axial value. Panel (c) is with anisotropic thermal conductivity.

An experiment is carried out to measure the rate of temperature change by inserting a thermocouple in the insulation. Heat capacity of the insulation is obtained from the manufacturer. From equation (9), it is found that heat flow into the insulation is very small, around 2% of the total heat generated by the flexible heater. As a result, this introduces additional uncertainty of around 2%. The effectiveness of insulation used in this work is further confirmed by the observation that a thermocouple suspended in vacuum just outside the heater does not register appreciable temperature rise.

A finite-element thermal simulation is carried out to determine the error introduced by heat conduction by the thin thermocouple and power supply wires. Simulation results indicate that due to the small diameter of the wires, less than 0.1% heat generated in the heater is lost in thermal conduction through the wires.

When accounting for all sources of uncertainty listed above, the total measurement uncertainty in the thermal conductivity and heat capacity values are estimated to be around $\pm 5\%$, also shown in Table 1.

5. Conclusions

This paper presents a simple method for measurement of thermophysical properties such as thermal conductivity and heat capacity of cylindrical Li-ion cells. By measuring the thermal response of the cell to an adiabatic heat flux into the cell in either radial or axial direction, it is possible to determine both radial and axial thermal conductivities in addition to heat capacity. The analytical model agrees well with finite-element simulations and has been validated against experimental data. The radial thermal conductivity is as low as $0.15\text{--}0.2\text{ W m}^{-1}\text{K}^{-1}$ for 26650 and 18650 cells. Measurements indicate strong thermal anisotropy in both cells tested in this work. The measured radial thermal conductivity is less than 1% of the measured axial thermal conductivity for 18650 and 26650 cells. This significantly large anisotropy has several important implications both for thermal modeling as well multi-physics modeling of physical phenomena that occur in a Li-ion cell. Not accounting for such anisotropy may lead to severe under-design or over-design of a Li-ion cell. By providing thermal property measurements, as opposed to thermal resistance measurements, this work contributes to a fundamental understanding of thermal transport within a Li-ion cell. The work may lead to improved thermal management solutions for Li-ion cells that ensure safety and reliability. In addition, due to the strong coupling

of thermal transport with other physical phenomena that occur in a Li-ion cell, this work may also lead to improved system-level performance and safety models.

Acknowledgments

Helpful discussions with Prof. Fuqiang Liu are gratefully acknowledged. This work was partially supported under ONR grants N00014-11-1-0659 and N00014-12-1-0594.

References

- [1] Q. Wang, P. Ping, X. Zhao, G. Chu, J. Sun, C. Chen, *J. Power Sources* 208 (2012) 210–224.
- [2] Z. Rao, S. Wang, *Renew. Sustain. Energy Rev.* 15 (2011) 4554–4571.
- [3] A.A. Pesaran, *J. Power Sources* 110 (2002) 377–382.
- [4] M. Kahn, K. White, R.T. Long, *Lithium-ion Batteries Hazard and Use Assessment*, Springer, 2011.
- [5] K. Smith, G.-H. Kim, E. Darcy, A. Pesaran, *Int. J. Energy Res.* 34 (2010) 204–215.
- [6] S.A. Khateeb, M.M. Farid, J.R. Selman, S. Al-Hallaj, *J. Power Sources* 128 (2004) 292–307.
- [7] W. Fang, O.J. Kwon, C.-Y. Wang, *Int. J. Energy Res.* 34 (2010) 107–115.
- [8] J.R. Belt, C.D. Ho, T.J. Miller, M.A. Habib, T.Q. Duong, *J. Power Sources* 142 (2005) 354–360.
- [9] Z. Ogumi, T. Abe, T. Fukutsuka, S. Yamate, Y. Iriyama, *J. Power Sources* 127 (2004) 72–75.
- [10] X.C. Zhang, A.M. Sastry, W. Shyy, *J. Electrochem. Soc.* 155 (2008) A542–A552.
- [11] G.-H. Kim, A. Pesaran, R. Spotnitz, *J. Power Sources* 170 (2007) 476–489.
- [12] B.Y. Liaw, E.P. Roth, R.G. Jungst, G. Nagasubramanian, H.L. Case, D.H. Doughty, *J. Power Sources* 119 (2003) 874–886.
- [13] D.G. Cahill, K.E. Goodson, A. Majumdar, *Trans. ASME J. Heat Transfer* 124 (2002) 223–241.
- [14] C. Forgez, D.V. Do, G. Friedrich, M. Morcrette, C. Delacourt, *J. Power Sources* 195 (2010) 2961–2968.
- [15] Y. Chen, J.W. Evans, *J. Electrochem. Soc.* 140 (1993) 1833–1838.
- [16] A. Mayyas, M. Omar, P. Pisu, A. Alahmer, C. Montes, *Int. J. Energy Res.* 37 (2011) 331–346.
- [17] S.C. Chen, C.C. Wan, Y.Y. Wang, *J. Power Sources* 140 (2005) 111–124.
- [18] T.M. Bandhauer, S. Garimella, T. Fuller, *J. Electrochem. Soc.* 158 (2011) R1–R25.
- [19] A.A. Pesaran, M. Keyser, *Thermal characteristics of selected EV and HEV batteries*, in: *Proc. Annual Battery Conf.: Advances & Applications*, Long Beach, CA, USA, 2001.
- [20] X. Lin, H.E. Perez, J.B. Siegel, A.G. Stefanopoulou, Y. Li, R.D. Anderson, Y. Ding, M.P. Castanier, *IEEE Trans. Control Syst. Technol.* 21 (2013) 1745–1755.
- [21] H. Maleki, S.A. Hallaj, J.R. Selman, R.B. Dinwiddie, H. Wang, *J. Electrochem. Soc.* 146 (1999) 947–954.
- [22] A. Jain, K.E. Goodson, *ASME Trans. J. Heat Transfer* 130 (2008) 1–7.
- [23] D.R. Lide, *Handbook of Organic Solvents*, CRC Press, Boca Raton, FL, 1994.
- [24] Y.S. Touloukian, *Thermophysical Properties of Matter*, 1st ed., IFI/Plenum, 1970.